Front. Chem. Sci. Eng. 2021, 15(1): 138–147
https://doi.org/10.1007/s11705-020-1935-8

RESEARCH ARTICLE

Effects of additive NaI on electrodeposition of Al coatings in $AlCl_3$-NaCl-KCl molten salts

Tianyu Yao[1,2], Haiyan Yang (✉)[1], Kui Wang[1], Haiyan Jiang (✉)[1], Xiao-Bo Chen[3], Hezhou Liu[2], Qudong Wang[1], Wenjiang Ding[1]

1 National Engineering Research Center of Light Alloy Net Forming, Shanghai Jiao Tong University, Shanghai 200240, China
2 The State Key Laboratory of Metal Matrix Composites, Shanghai Jiao Tong University, Shanghai 200240, China
3 School of Engineering, RMIT University, Melbourne, VIC 3000, Australia

Abstract Effects of NaI as an additive on electrodeposition of Al coatings in $AlCl_3$-NaCl-KCl (80-10-10 wt-%) molten salts electrolyte at 150 °C were investigated by means of cyclic voltammetry, chronopotentiometry, scanning electron microscopy and X-ray diffraction (XRD). Results reveal that addition of NaI in the electrolyte intensifies cathodic polarization, inhibits growth of Al deposits and increases number density of charged particles. The electrodeposition of Al coatings in the $AlCl_3$-NaCl-KCl molten salts electrolyte proceeds via three-dimensional instantaneous nucleation which however exhibits irrelevance with NaI. Galvanostatic deposition results indicate that NaI could facilitate the formation of uniform Al deposits. A compact coating consisting of Al deposits with an average particle size of 3 μm was obtained at a current density of 50 $mA \cdot cm^{-2}$ in $AlCl_3$-NaCl-KCl molten salts electrolyte with 10 wt-% NaI. XRD analysis confirmed that NaI could contribute to the formation of Al coating with a preferred crystallographic orientation along (220) plane.

Keywords NaI, additive, electrodeposition, molten salts, Al coating

1 Introduction

Aluminum coatings on the surface of metal substrates have attracted widespread attention by virtue of their high resistance to corrosion and high-temperature oxidation [1,2]. Spraying coating [3], liquid diffusion [4], aluminizing [5], high energy beam cladding [6], vapor deposition [7,8] and electrodeposition are the main methods to deposit Al coatings on metal substrate. Among them, electrodeposition attracts increasing attention owing to the ease in operation, cost-effectiveness and being applicable to substrates with irregular geometries [9]. Thickness and quality of such Al coatings can be tailored through optimization of the processing parameters of electrodeposition.

Given the technical challenges associated with the electrodeposition of Al coatings in aqueous solutions, a number of non-aqueous electrolytes have been developed [10–13]. Non-aqueous electrolytes suitable for Al electrodeposition fall into three categories: (i) organic solvents, mixtures of Al $(C_2H_5)_3$ or AlX_3 (X = Br or Cl) with NaF or $LiAlH_4$ dissolved in organic solvents; (ii) ionic liquids, mixtures of AlX_3 (X = Br or Cl) with various organic halide salts; and (iii) molten salts (inorganic), mixtures of AlX_3 (X = Br or Cl) with alkali metals halide salts. Organic solvents in general own severe volatility and incur significant pollution, whilst poor stability and high production cost are main drawbacks of ionic liquids. As such, molten salts can be taken as a promising candidate for electroplating Al coating due to their cost effectiveness, simple processing requirements and long lifespan of the electrolytes.

A large number of studies have focused on the electrodeposition of Al and Al alloy coatings in $AlCl_3$-NaCl-KCl molten salts due to their low eutectic point [14]. Al-Mn, Al-Mg, Al-Cu, Al-Pt, Al-Sn, Al-Nb, Al-Zr, Al-Ta, Al-Sb, Al-Bi, Al-Te, Al-Cr-Ni [15–24] and other binary or ternary alloys were successfully synthesized by incorporating corresponding metal ions into the electrolytes. Various substrate materials, such as graphite, steel, brass, tungsten, molybdenum and gold were also adopted and investigated [17,20,25–28]. However, it remains a chal-

Received October 29, 2019; accepted March 11, 2020

E-mails: yanghaiyan@sjtu.edu.cn (Yang H),
jianghy@sjtu.edu.cn (Jiang H)

lenge to avoid the formation of Al dendrites and micro-holes in the Al deposits to yield uniform and smooth Al and Al alloy coatings due to high deposition temperature. In particular, with increasing thickness of Al deposits, the presence of dendrites and micro-holes makes the electrodeposition Al and Al alloy coatings more vulnerable to rupture and detachment from substrate, which impedes further applications. In addition to the sophisticated controls over the electrodeposition parameters, current density, potential and temperature, appropriate additives are essential to electroplating compact and dense Al coatings in molten salts for high quality Al and Al alloy coatings [29,30].

Though enormous effort has been devoted to the development of sound additives for metal electrodeposition in aqueous solutions, only a few studies focus on additives for the electrodeposition of Al in non-aqueous solutions, especially in molten salts [31,32]. Additives for Al electrodeposition mainly depend on electrolytes since there are considerable discrepancies in solubility. Additives in organic solvents and ionic liquids electrolytes are usually small molecule compounds, such as amines, pyridines and nicotinamides [33,34]. Small organic molecules, such as nicotinic acid and methyl nicotinate, could improve Al coatings significantly [35]. While, some small ionic and inorganic molecules are usually added in molten salts electrolytes. Research shows that hydrogen halides, e.g., hydrogen chloride, could contribute to the formation of coherent and dendrite-free Al coating in $AlCl_3$-NaCl molten salts [36]. However, hydrogen halides are volatile and difficult to control when added into molten salts electrolytes. Besides, sulfides were confirmed to prevent the formation of Al dendrites in a $NaAlCl_4$ molten salt electrolyte [37], but their poor solubility limits further application. Alkali halides, such as LiCl, KCl, NaBr, NaI, KI, and so on, were found to be favorable alternatives as effective additives in electrodeposition of Al due to their solubility and low volatility [29,30,32,38–40], LiCl and KCl were proven to be beneficial to the formation of high-quality Al coatings [29,30]. KI was found to be an effective surfactant in electrodeposition of Al [38,39] and addition of NaI shows improvement in the quality of deposited Al layers [40]. However, most researches have focused on the effect of alkali halides on morphologies and properties, few have focused on mechanism. Some researchers tried to unveil the working mechanism of alkali halide through studying different speciation of Al in molten salts [32]. In order to in-depth understand the mechanism of additives and further improve the Al coatings' quality, a systematic study of electrochemical behavior and nucleation/growth mechanism is of great significance.

Hence, in the present study, we focus on the effects of NaI on deposition mechanism, morphology and microstructure of Al from $AlCl_3$-NaCl-KCl (80-10-10 wt-%) molten salts electrolyte. The effects of NaI on the electrochemical behavior and the deposition mechanism of Al were investigated by cyclic voltammetry (CV) and chronoamperometry (CP). Electrodeposits were characterized using scanning electron microscopy (SEM) and X-ray diffraction (XRD).

2 Experimental

2.1 Preparation of molten salt electrolytes

Sodium chloride and potassium chloride (NaCl and KCl, AR, 99.9% purity, Sinopharm Chemical Reagent Co. Ltd., China) were initially dried at 300 °C for 72 h in a vacuum drying chamber. Anhydrous Al chloride ($AlCl_3$, AR, 99.8% pure, Sinopharm Chemical Reagent Co., Ltd., China) and sodium iodide (NaI, AR, 99.5%, Macklin) were used as received. A mixture of $AlCl_3$, NaCl and KCl (80-10-10 wt-%) was melted at 150 °C in a radius flask on a temperature-controlled heater inside a glove box (Mikrouna Upure 1220/750/900, China). All the electrochemical and electrodeposition experiments were carried out in a glove box with a protective Ar atmosphere. To study the effects of NaI on electrodeposition of Al, NaI was added into the molten salts and then continuously stirred for 4 h with a magnetic stirrer to yield a homogeneous light-yellow solution.

2.2 Electrochemical tests

All electrochemical experiments were conducted using an electrochemical workstation (CHI655D, Shanghai Chenhua Device Company, China) with a typical three-electrode cell. A glassy carbon disc (GC, 0.07 cm^2) was used as working electrode. An Al plate (99.9%, 350 mm^2, Alfa Aesar) was used as counter electrode. A pure Al wire (99.9%, Φ 0.5 mm, Alfa Aesar) placed in a small Pyrex glass tube filled with $AlCl_3$-NaCl-KCl (80-10-10 wt-%) molten salts was used as reference electrode. The counter and reference electrodes were polished with emery papers, cleaned in an ultrasonic bath for 3 min and rinsed with distilled water, then dried in a vacuum drying chamber before all measurements. CV were performed at a scan rate of 50 $mV \cdot s^{-1}$.

2.3 Electrodeposition

For electrodeposition, an Al wire and plate as described above were used as reference electrode and anode, respectively. A Cu foil (99.9%, 5 mm × 5 mm, Aldrich) was connected as cathode. The distance between cathode and anode was maintained at 10 mm. The Cu foil, Al plate and wire were cleaned and dried before being transferred into the glove box as described in preparation of molten salt electrolytes. Cathodic deposition of Al was performed using a constant current mode at 150 °C. The current density was set at 50 $mA \cdot cm^{-2}$, and the process of

electrodeposition last for 10 min. After electrodeposition, the samples were thoroughly cleaned with anhydrous acetone in an ultrasonic bath for two minutes and rinsed with distilled water and then dried in a vacuum drying chamber.

2.4 Characterization of the electrodeposition Al coatings

Surface and cross-sectional morphology of the Al coatings was observed using field emission scanning electron microscopy (SIRION200, FEI, US). Samples were examined by XRD (D/MAX2000 V, Rigaku, Japan) to identify possible constituents and crystallographic structure. $2\theta/\theta$ scanning mode was executed over a $2\theta = 30° - 80°$ range with a scanning speed of $5° \cdot \text{min}^{-1}$ with a step of 0.01°.

3 Results and discussion

3.1 Voltammetric behavior

The CV of Al on the GC electrode in the $AlCl_3$-NaCl-KCl (80-10-10 wt-%) molten salts electrolyte at 150 °C are shown in Fig. 1.

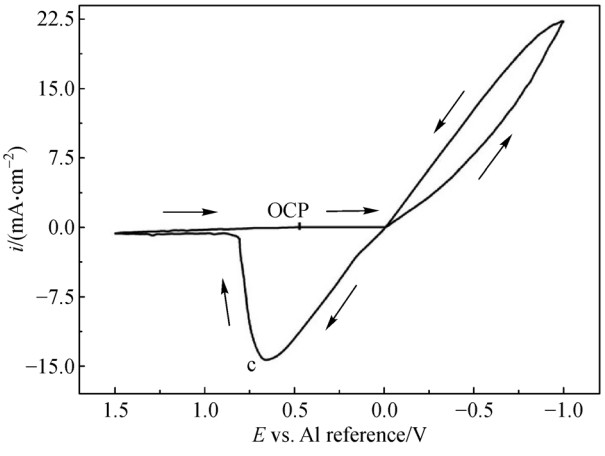

Fig. 1 The cyclic voltammogram recorded on a GC electrode at 50 $mV \cdot s^{-1}$ in the $AlCl_3$-NaCl-KCl (80-10-10 wt-%) molten salts electrolyte, at 150 °C.

The electrode potential was scanned from open circuit potential (OCP) in the potential ranging from 1.50 to −1.00 V (vs. Al/Al^{3+}). The scan rate was set at 50 $mV \cdot s^{-1}$. As shown in Fig. 1, when the potential was scanned from the OCP to −1.00 V (vs. Al/Al^{3+}), a rising cathodic current with onset potential at approximately 0.00 V (vs. Al/Al^{3+}) was ascribed to the bulk electrodeposition of Al. As the potential shifted from 0.00 V to −1.00 V, Al^{3+} ions were reduced and deposited on the cathode electrode continuously. And no peak was found in the CV curve (Fig. 1) suggesting that only one electrodeposition reaction occurred, as following Eq. (1), according to the composition of the electrolyte in which the main type of ions is $Al_2Cl_7^-$:

$$4Al_2Cl_7^- + 3e^- \rightleftharpoons Al \downarrow + 7AlCl_4^- \quad (1)$$

In the reverse scan, a crossing current loop is observed, which indicates that the electrodeposition of Al on GC electrode involves a nucleation/growth process. Such phenomena usually could be found in the electrodeposition of a metal on a foreign metal substrate [41]. An anodic wave with peak potential at approximately 0.70 V (vs. Al/Al^{3+}) is observed (peak c), and this anodic current density peak can be attributed to the Al stripping. In addition, an obvious oxidation peak but no reduction peak was observed in the CV curve. And there were still some Al deposits found on the surface of GC electrode when the CV experiment was finished. All these indicate that the electrodeposition of Al in $AlCl_3$-NaCl-KCl molten salts is irreversible.

To investigate the effect of NaI on the voltammetric behavior of Al, CV curves were carried out in $AlCl_3$-NaCl-KCl (80-10-10 wt-%) molten salts electrolyte with different amount of NaI on a GC electrode. Each voltammogram was recorded on a fresh GC electrode surface. The CV curves in $AlCl_3$-NaCl-KCl molten salts electrolyte with 0, 1, 5 and 10 wt-% NaI are shown in Fig. 2.

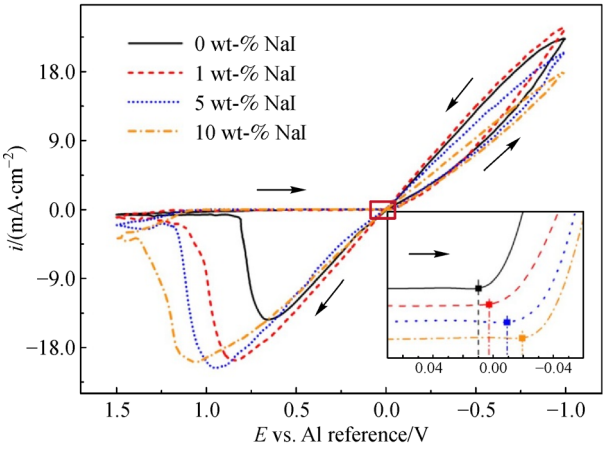

Fig. 2 The CV recorded on a GC electrode at 50 $mV \cdot s^{-1}$ in the $AlCl_3$-NaCl-KCl (80-10-10 wt-%) molten salts electrolyte containing 0, 1, 5 and 10 wt-% NaI, respectively, at 150 °C.

The addition of 1 wt-% NaI into the electrolyte increased the cathodic current density, since the introduction of a little NaI might increase the number of conductive ions, so that the conductivity of the electrolyte was increased, which would promote the electrodeposition of Al. However, when 5 or 10 wt-% NaI was introduced into the electrolyte, the cathodic current density decreased, indicating that a certain amount of NaI could give rise to an

inhibition of Al deposition. Previous studies have shown that the I^- could be absorbed on the electrode surface to inhibit the cathodic reduction reaction [38].

As shown in the inset of Fig. 2, the reduction potential of cathodic shifts slightly towards negative direction with the increase of NaI, implying that NaI intensifies the cathodic polarization. Generally, appropriate polarization is necessary in electrodeposition since a sufficiently high overpotential is required for nucleation. Thus, the addition of NaI intensifies the cathodic polarization and inhibits the growth of Al deposits, which is helpful to form a smooth electrodeposition coating (as shown in Fig. 6). A reasonable explanation of the effect of the addition is that the I^- ions ionized from NaI function as a surfactant and its adsorption on the electrode surface promotes nucleation and inhibits reduction of Al^{3+} [38]. Besides, the anodic current density peak shifts towards the positive direction and the anodic charge increases as NaI content increases. This means that Al could be more easily dissolved when NaI is added into the electrolyte. It is inferred that NaI may be used as a useful auxiliary in the anodic dissolution industry.

3.2 Chronoamperometric investigations

In order to further study the effect of NaI on Al nucleation and growth in $AlCl_3$-NaCl-KCl molten salts electrolyte, chronoamperometric experiments were performed on a GC electrode immediately after short induction time. The potential varied from a value where no reduction of Al^{3+} took place to a more negative value where the nucleation and growth of Al particles would be initiated. The experiments were carried out in the $AlCl_3$-NaCl-KCl molten salts electrolyte with 0, 1, 5 and 10 wt-% NaI, and a series of representative current-time transients resulting from these experiments are shown in Fig. 3.

In spite of the different content of NaI, the presence of the peaks in the potential step current transients is normally associated with nucleation/growth process. As the potential is relatively positive, there is no reaction of Al^{3+} occurring in the molten salt electrolyte, the current is stable. With the increase of potential, the nucleation and growth of Al particles would be initiated. The trend of the current as a function of potential shows the process of the formation and growth of Al nuclei. There is an obvious

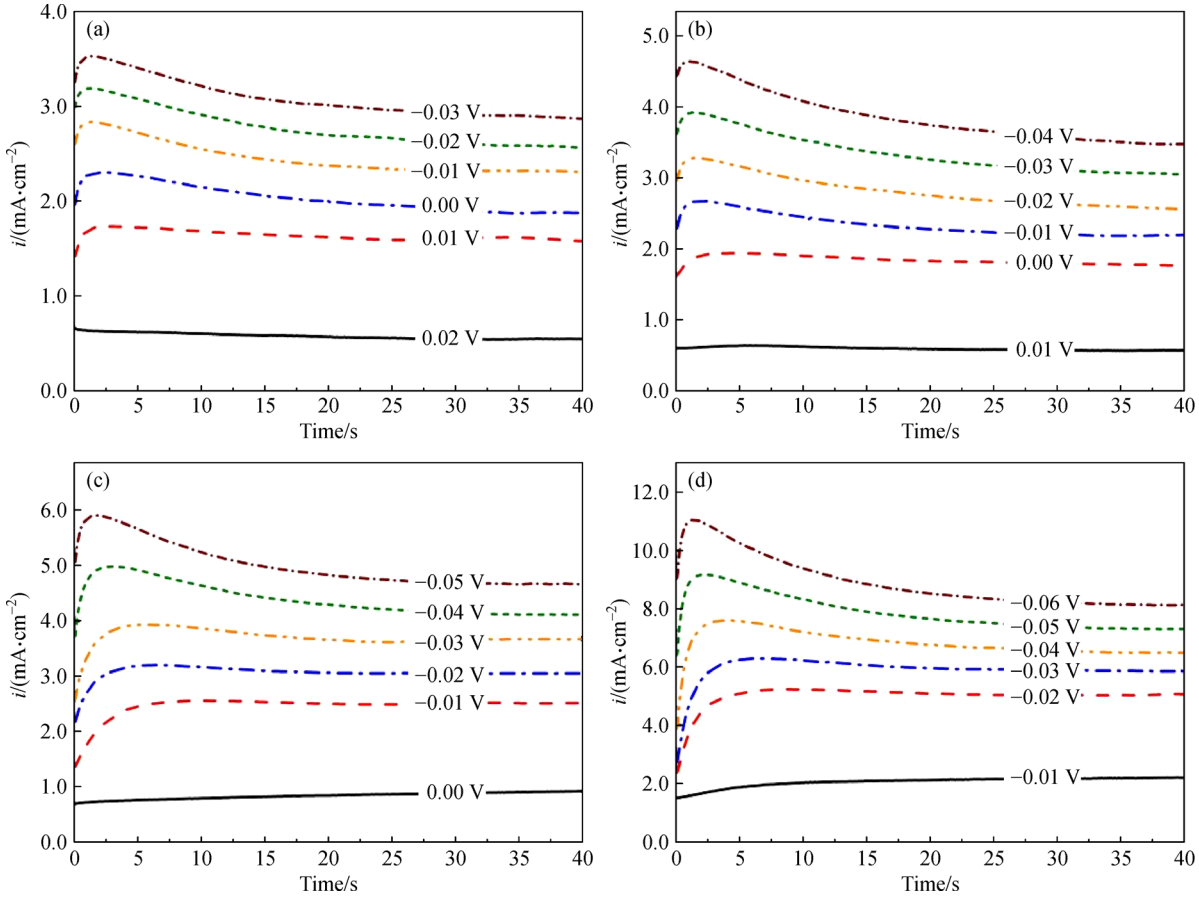

Fig. 3 The typical current-time transients resulting from these experiments in the $AlCl_3$-NaCl-KCl molten salts electrolyte with (a) no NaI, (b) 1 wt-% NaI, (c) 5 wt-% NaI, (d) 10 wt-% NaI.

current peak in each current curve due to the formation and growth of Al nuclei which makes Al ions collected. When the overlap [42] occurs, the increasing current reaches the maximum, i_m, and the peak is formed at the time, t_m. Afterwards, almost all the current values decrease owning to the consumption of $Al_2Cl_7^-$. As the potential applied increases, the i_m becomes higher while the t_m becomes shorter. It means that the time required to overlap decreases as the nucleation density increases. Additionally, the current transients do not have the tendency to converge to an accordant value over time, and the stable values of current density increase as the potential applied increases. This implies that the electrodeposition of Al in $AlCl_3$-NaCl-KCl molten salts electrolyte is controlled by electrochemical reaction rather than diffusion, which is usually observed in most ionic liquids due to the lack of reductive ions around the cathode electrode [43]. It is quite reasonable since there are abundant $Al_2Cl_7^-$ ions in an $AlCl_3$-NaCl-KCl (80-10-10 wt-%) molten salts electrolyte.

Taking the content of NaI into consideration, it can be found that the potential under which the reduction of Al^{3+} took place (as indicated by the red curves in Fig. 3) became more negative when NaI was added. It illustrates that the addition of NaI increases the overpotential of electrodeposition and promotes the cathodic polarization. The results agree well with those of the above voltammograms, and it also reveals that the peak current densities of the *i-t* curves under the same potential increase with the increasing NaI additions. It may be because that the addition of NaI increases number density of charged particles in the electrolyte and conductivity of the electrolyte rises.

Normally, there are two mechanisms [44] of additives adopted for electroplating: (1) make it more difficult to nucleate metal clusters by complexing the metal ions and increasing their reduction potential; (2) inhibit nucleation and restrict growth by adsorption on the electrode surface. Based on the above results, the latter may be the main mechanism of NaI. I^- ions ionized from NaI could block active sites on the cathode surface, increase the number of growing nuclei and inhibit the growth of nuclei, leading to an energetic homogenization of the surface. The introduction of NaI increases the conductivity of the electrolyte and promotes electrodeposition.

The electrodeposition of metals or alloys onto a metal substrate often involves some types of three-dimensional nucleation process accompanied with hemispherical growth of the developing nuclei. There are two different models of three-dimensional nucleation/growth, described as 'instantaneous', and 'progressive' [45]. The instantaneous model refers to the situation in which a fixed number of nucleation sites are all activated at the same time after the potential step, whereas progressive model refers to the situation in which the nucleation sites gradually become activated as the chronoamperometric experiment proceeds. In this system, the two differentiating nucleation models can be obtained by comparison of the dimensionless experimental current-time transients to the dimensionless theoretical transients. The theoretical transients for limiting cases of instantaneous (Eq. (2)) and progressive (Eq. (3)) nucleation are represented, respectively, by

$$\left(\frac{i}{i_m}\right)^2 = \frac{1.9542}{t/t_m}\left\{1-\exp\left[-1.2564\left(\frac{t}{t_m}\right)\right]\right\}^2, \quad (2)$$

$$\left(\frac{i}{i_m}\right)^2 = \frac{1.2254}{t/t_m}\left\{1-\exp\left[-2.3367\left(\frac{t}{t_m}\right)^2\right]\right\}^2. \quad (3)$$

To clarify the influence mechanism of NaI on the nucleation/growth, the data from the chronoamperometric experiments are normalized and compared with the theoretical transients. Figure 4 shows the experimental and theoretical plots of $(i/i_m)^2$ vs (t/t_m) with different content of NaI.

Compared with the theoretical model, the experimental plots are all in good agreement with instantaneous nucleation model, suggesting that the electrodeposition of Al can be regarded as instantaneous nucleation. It indicates that the electrodeposition of Al coatings on Cu electrode in the $AlCl_3$-NaCl-KCl molten salts electrolyte proceeds via three-dimensional instantaneous nucleation, which however exhibits irrelevance with NaI.

3.3 Electrodeposition and characterization of Al deposits

Different current densities were applied to the electrodeposition of Al to study the effect of current densities on the morphologies of Al coatings. Figures 5(a), 5(b) and 5(c) show the SEM images of the Al deposits obtained in $AlCl_3$-NaCl-KCl (80-10-10 wt-%) molten salts without NaI at three different current densities of 25, 50 and 75 $mA \cdot cm^{-2}$, respectively. It can be seen that when the current density was 25 $mA \cdot cm^{-2}$, only a few discrete large crystal particles were formed on the Cu substrate. When the current density was increased to 50 $mA \cdot cm^{-2}$, a continuous layer of Al coating was formed. Al particles became small and homogeneous, whose average size was about 7 μm. Further increasing the current density to 75 $mA \cdot cm^{-2}$, the Al deposits became non-uniform and irregular, and the electrodeposition Al coating was rough and loose. Besides, the high current density will damage the electrolyte, causing the decomposition of the electrolyte. Therefore, 50 $mA \cdot cm^{-2}$ was adopted as a suitable current density for the electrodeposition of Al. The EDXS spectrum of the Al electrodeposits is presented in Fig. 5(d). It shows a strong peak of Al, meaning that the main constituent of the coating is Al. The results reveal the spectrum of the Al includes a weak peak of Cu and a tiny peak of O. The Cu peak should be attributed to the Cu substrate, indicating that the electrodeposition Al coatings obtained from molten salts without NaI were loose and the

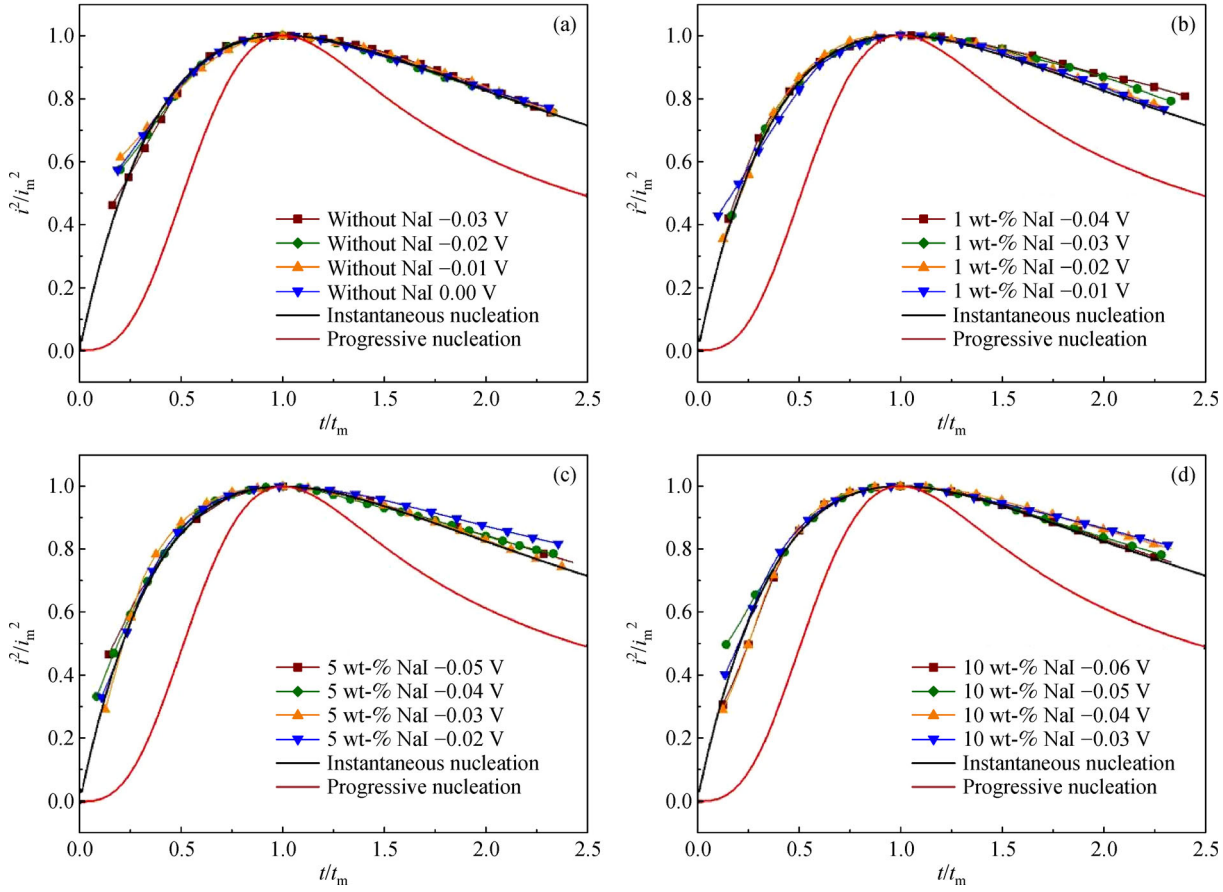

Fig. 4 Comparison of the experimental and theoretical plots of $(i/i_m)^2$ vs. (t/t_m) in the $AlCl_3$-NaCl-KCl molten salts electrolyte with (a) no NaI, (b) 1 wt-% NaI, (c) 5 wt-% NaI and (d) 10 wt-% NaI.

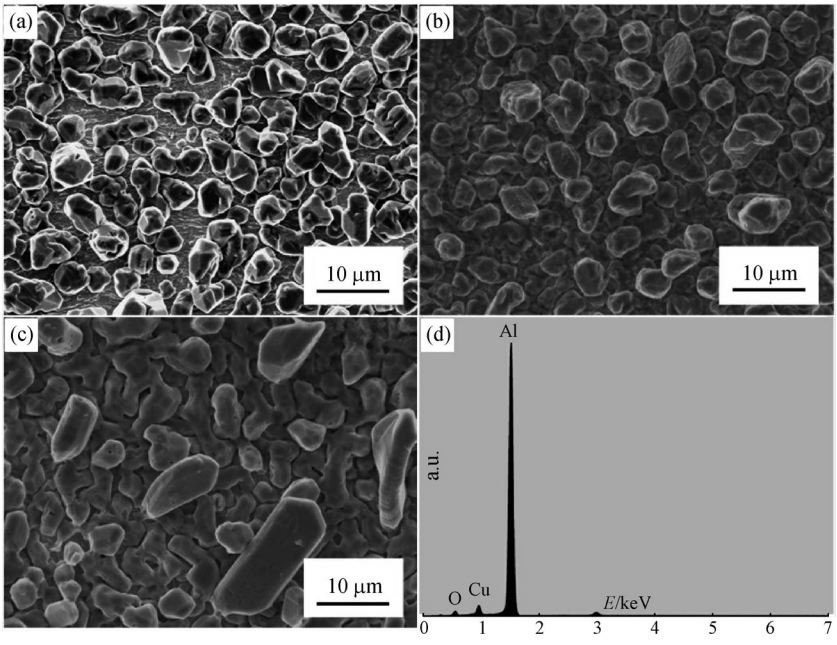

Fig. 5 The microscopic morphologies of the Al electrodeposits obtained on a copper foil in the $AlCl_3$-NaCl-KCl (80-10-10 wt-%) molten salts at 150 °C and (a) 25 $mA \cdot cm^{-2}$, (b) 50 $mA \cdot cm^{-2}$, (c) 75 $mA \cdot cm^{-2}$, and (d) the typical energy dispersive X-ray spectrometer (EDXS) spectrum of the Al electrodeposits.

thickness was non-uniform. While the O peak is probably because the surface of the electrodeposition Al coating was oxidized when it was exposed in the air.

Al deposited samples in $AlCl_3$-NaCl-KCl molten salts electrolyte with various NaI concentration at 150 °C at the current density of 50 mA·cm^{-2} were examined by SEM and EDXS (Fig. 6). When 1 wt-% NaI was added into the electrolyte, the Al particles got smaller but the surface was still rough, and the particle sizes were non-uniform (Fig. 6(a)). With the increase of the NaI content to 5 wt-%, the surface became dense and compact (Fig. 6(b)), but the particle sizes were still non-uniform. As the NaI content reached 10 wt-%, a compact and uniform electrodeposition Al coating was achieved (Fig. 6(c)). Compared with the samples obtained in the electrolytes without NaI, the particle size of the Al deposits became much smaller. The average particle size of the Al coatings decreases to approximately 3 μm, indicating that NaI is of great help in refining the particle size of the Al deposits. As shown in Fig. 6(d), no peak of Cu or O was detected in the Al coating, indicating that the Al coatings became dense and their thickness became uniform electrodeposited from the electrolyte with the addition of NaI, so the Cu peak detected from the substrate disappeared. The EDXS results demonstrate that the deposits are essentially composed of pure Al and free of the molten salts electrolyte, and that the electrodeposition Al coatings obtained from $AlCl_3$-NaCl-KCl molten salts electrolyte by NaI were of high quality.

The cross-sectional morphologies of the Al coatings deposited from the $AlCl_3$-NaCl-KCl molten salts electrolyte with 0, 1, 5 and 10 wt-% NaI are shown in Fig. 7. As shown in Fig. 7, the cross-sectional morphologies of the Al coatings were dependent on the content of NaI. The thickness of the Al coating electrodeposited from the electrolyte without NaI is non-uniform with a range of 2.5–10 μm. That is why a weak Cu peak can be detected from the sample electrodeposited from the electrolyte without NaI in Fig. 5(d). The thickness of the Al coatings obviously became even and uniform when NaI was added into the electrolyte. When 1 wt-% NaI was added, the thickness at the thinnest site was approximately 4 μm and it increased to 5–6 μm when 5 or 10 wt-% NaI was added into the electrolyte, as marked by the dotted line in the cross-sectional morphologies. The uniformity in thickness of a coating is vital to its protection, since the failures usually preferentially occur at its thinnest site. Otherwise, the Al coatings all exhibited good adhesion with Cu substrates.

The cathodic current efficiency was measured based on the mass of the electrodeposited Al and calculated using Faraday's law, the current efficiency of the Al coatings obtained from the $AlCl_3$-NaCl-KCl molten salts electrolyte with 10 wt-% NaI reached 98%.

XRD analysis was performed to further characterize the microstructure of the Al coating and the XRD patterns of the Al-deposited samples are shown in Fig. 8(a). All the strong diffraction peaks in the pattern can be identified as Al and the Cu substrate. The obtained Al electrodeposit exhibits four clear diffraction peaks (111), (200), (220), and (311), indicating that the Al coatings are compose of fcc Al. In order to study the effect of NaI on the orientation of Al coatings, the texture co-efficient (*TC*) was adopted

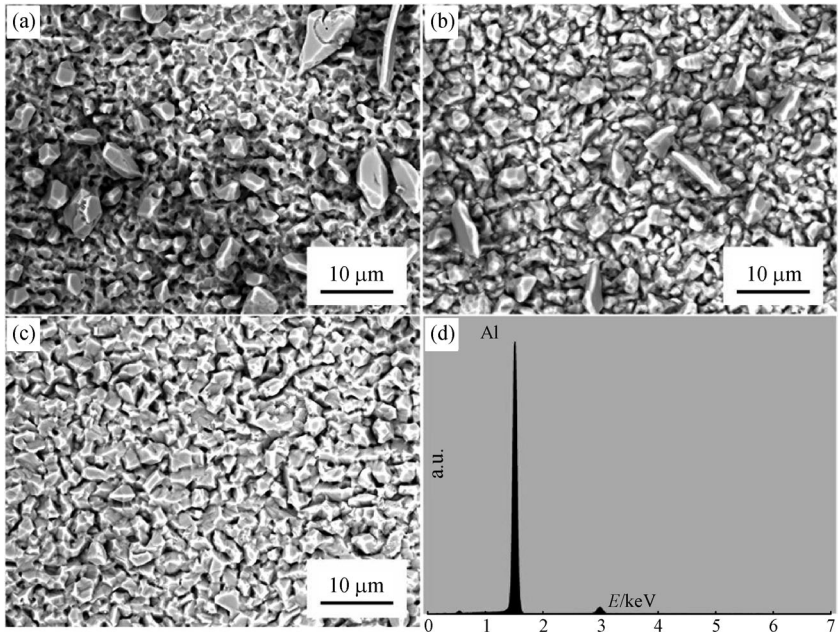

Fig. 6 The microscopic morphologies of the Al electrodeposits obtained on a copper foil in the $AlCl_3$-NaCl-KCl (80-10-10 wt-%) molten salts electrolyte at 25 mA·cm^{-2} and 150 °C with (a) 1 wt-% NaI, (b) 5 wt-% NaI, (c) 10 wt-% NaI, and (d) the typical EDXS spectrum of the Al electrodeposits.

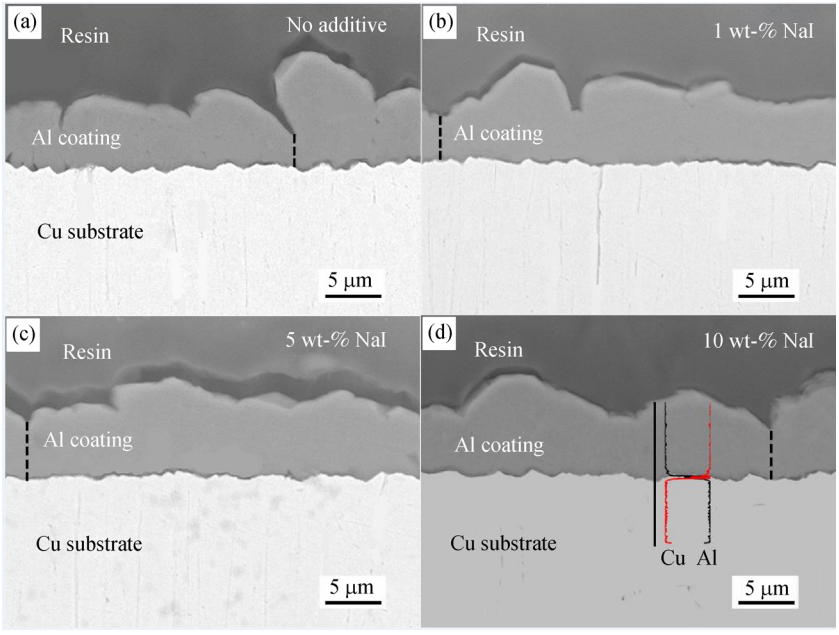

Fig. 7 The cross-sectional morphology of the Al coating deposited from the electrolyte with (a) no NaI, (b) 1 wt-% NaI, (c) 5 wt-% NaI and (d) 10 wt-% NaI.

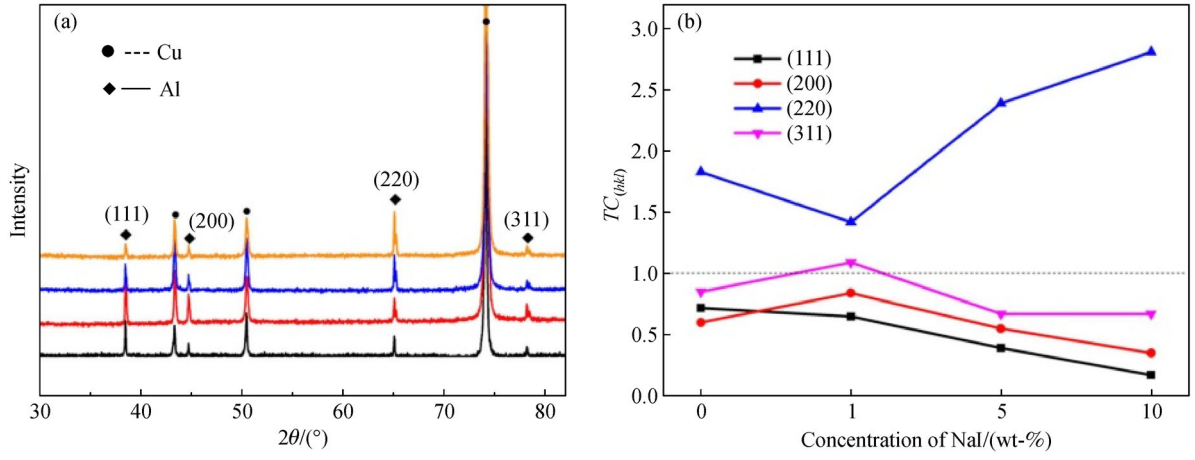

Fig. 8 (a) The XRD patterns of the electrodeposition Al coating on a copper foil in $AlCl_3$-NaCl-KCl (80-10-10 wt%) molten salts electrolyte with 0, 1%, 5%, 10% NaI and (b) the *TC* values calculated from XRD reflections.

and calculated by following equations [46]:

$$TC_{(hkl)} = \frac{I_{(hkl)} / \sum I_{(hkl)}}{\frac{1}{n} \sum Ir_{(hkl)} / Ir_{(hkl)}}, \quad (4)$$

where $I_{(hkl)}$ is the peak intensity of the (*hkl*) for the obtained samples; $Ir_{(hkl)}$ is the peak intensity of the (*hkl*) crystallographic plane for the JCPDS card No. 00-004-0787, and *n* is the total number of diffractions. The orientations of Al coatings are out of order when the *TC* values of different crystal faces are equal, and a larger *TC* value of crystal face means more preferred orientations. The *TC* values of Al coatings obtained in $AlCl_3$-NaCl-KCl molten salts with different content of NaI at 150 °C are calculated based on Eq. (4) and the results are listed in Fig. 8(b). It can be seen that all of the deposits have a preferred (220) orientation. The *TC* values of (311) are very close to 1.0, indicating that the (311) intensity is equal to that of a randomly oriented sample. The other two orientations, (200) and (111), have the relatively weak diffraction intensities. As the concentration of NaI increases, the intensity of (220) increases dramatically, while the relative intensities of orientation (111), (200) and (311) decrease. It can be inferred that NaI could contribute to the formation of a preferred crystallographic orientation along (220) plane.

4 Conclusions

Al was successfully electrodeposited from $AlCl_3$-NaCl-KCl (80-10-10 wt-%) molten salts electrolyte at 150 °C with NaI addition, and the effects of NaI on the electrodeposition of Al were studied by CV and CP investigations. It shows that NaI intensifies the cathodic polarization and produces an inhibition effect on Al deposition on the electrode surface. The electrodeposition of Al on a Cu electrode in $AlCl_3$-NaCl-KCl (80-10-10 wt-%) molten salts electrolyte proceeds via three-dimensional instantaneous nucleation, and the nucleation/growth process was not affected by NaI. NaI could increase the conductivity and promote the refinement of the particle size, contributing to the formation of a continuous and uniform layer of Al coating.

A compact layer of electrodeposited Al coating was obtained at a current density of 50 $mA \cdot cm^{-2}$ with 10 wt-% NaI. The average particle size was approximately 3 μm and the average thickness of the obtained Al layer was approximately 10 μm. NaI could contribute to the formation of a preferred crystallographic orientation along (220) plane.

Acknowledgements The authors would gratefully acknowledge the financial support from the National Natural Science Foundation of China (Grant No. 51301110), China Postdoctoral Science Foundation (No. 2016M600311), Science and Technology Innovation Action Plan—International Enterprises Science and Technology Cooperation Program of Shanghai (No. 17230732700).

References

1. Aguero A, Gutierrez M, Muelas R. Aluminum solid-solution coating for high-temperature corrosion protection. Oxidation of Metals, 2017, 88(1-2): 145–154
2. Dai J J, Li S Y, Zhang H X, Yu H J, Chen C Z, Li Y. Microstructure and high-temperature oxidation resistance of Ti-Al-Nb coatings on a Ti-6Al-4V alloy fabricated by laser surface alloying. Surface and Coatings Technology, 2018, 344: 479–488
3. Wang Q, Sun Q, Zhang M X, Niu W J, Tang C B, Wang K S, Rui X, Zhai L, Wang L. The influence of cold and detonation thermal spraying processes on the microstructure and properties of Al-based composite coatings on Mg alloy. Surface and Coatings Technology, 2018, 352: 627–633
4. Belova I V, Heuskin D, Sondermann E, Ignatzi B, Kargl F, Murch G E, Meyer A. Combined interdiffusion and self-diffusion analysis in Al-Cu liquid diffusion couple. Scripta Materialia, 2018, 143: 40–43
5. Cho L, Seo E J, Sulistiyo D H, Jo K R, Kim S W, Oh J K, Cho Y R, De Cooman B C. Influence of vanadium on the hydrogen embrittlement of aluminized ultra-high strength press hardening steel. Materials Science and Engineering A, 2018, 735: 448–455
6. Luo X X, Yao Z J, Zhang P Z, Gu D D. Al_2O_3 nanoparticles reinforced Fe-Al laser cladding coatings with enhanced mechanical properties. Journal of Alloys and Compounds, 2018, 755: 41–45
7. Christoglou Ch, Voudouris N, Angelopoulos G N, Pant M, Dahl W. Deposition of aluminum on magnesium by a CVD process. Surface and Coatings Technology, 2004, 184(2): 149–155
8. Meng F P, Peng S, Xu G B, Wang Y, Ge F F, Huang F. Structure of uniform and high-quality Al-doped ZnO films by magnetron sputter deposition at low temperatures. Thin Solid Films, 2018, 665: 109–116
9. Gamburg Y D, Zangari G. Theory and Practice of Metal Electrodeposition. Heidelberg: Springer, 2011, 1–2
10. Landolt D. Electrodeposition science and technology in the last quarter of the twentieth century. Journal of the Electrochemical Society, 2002, 149(3): S9–S20
11. Gu Y K, Liu J, Qu S X, Deng Y D, Han X P, Hu W B, Zhong C. Electrodeposition of alloys and compounds from high-temperature molten salts. Journal of Alloys and Compounds, 2017, 690: 228–238
12. Zhao Y G, VanderNoot T J. Electrodeposition of aluminium from nonaqueous organic electrolytic systems and room temperature molten salts. Electrochimica Acta, 1997, 42(1): 3–13
13. Liu F, Deng Y D, Han X P, Hu W B, Zhong C. Electrodeposition of metals and alloys from ionic liquids. Journal of Alloys and Compounds, 2016, 654: 163–170
14. Simka W, Puszczyk D, Nawrat G. Electrodeposition of metals from non-aqueous solutions. Electrochimica Acta, 2009, 54(23): 5307–5319
15. Zhang J F, Yan C W, Wang F H. Electrodeposition of Al-Mn alloy on AZ31B magnesium alloy in molten salts. Applied Surface Science, 2009, 255(9): 4926–4932
16. Li Y L, Zhao P, Dai Y H, Yao M Q, Gan H B, Hu W C. Electrochemical deposition of Al-Mg alloys on tungsten wires from $AlCl_3$-NaCl-KCl melts. Fusion Engineering and Design, 2016, 103: 8–12
17. Li W, Chen Z, Wei C C, Kong W P, Xu B H, Jia X Y, Diao C L, Li S J. The electrochemical formation of Al-Cu alloys in a LiCl-KCl-$AlCl_3$ molten salt. Electrochimica Acta, 2016, 196: 162–168
18. Ueda M, Hayashi H, Ohtsuka T. Electrodeposition of Al-Pt alloys using constant potential electrolysis in $AlCl_3$-NaCl-KCl molten salt containing $PtCl_2$. Surface and Coatings Technology, 2011, 205(19): 4401–4403
19. Ueda M, Inaba R, Ohtsuka T. Composition and structure of Al-Sn alloys formed by constant potential electrolysis in an $AlCl_3$-NaCl-KCl-$SnCl_2$ molten salt. Electrochimica Acta, 2013, 100: 281–284
20. Vukićević N M, Cvetković V S, Jovanović L, Stevanović S, Jovićević J N. Alloy formation by electrodeposition of niobium and aluminium on gold from chloroaluminate melts. International Journal of Electrochemical Science, 2017, 12: 1075–1093
21. Ueda M, Teshima T, Matsushima H, Ohtsuka T. Electroplating of Al-Zr alloys in $AlCl_3$-NaCl-KCl molten salts to improve corrosion resistance of Al. Journal of Solid State Electrochemistry, 2015, 19 (12): 3485–3489
22. Sato K, Matsushima H, Ueda M. Electrodeposition of Al-Ta alloys in NaCl-KCl-$AlCl_3$ molten salt containing $TaCl_5$. Applied Surface Science, 2016, 388: 794–798
23. Ebe H, Ueda M, Ohtsuka T. Electrodeposition of Sb, Bi, Te, and their alloys in $AlCl_3$-NaCl-KCl molten salt. Electrochimica Acta, 2007, 53(1): 100–105

24. Ueda M, Kigawa H, Ohtsuka T. Co-deposition of Al-Cr-Ni alloys using constant potential and potential pulse techniques in $AlCl_3$-NaCl-KCl molten salt. Electrochimica Acta, 2007, 52(7): 2515–2519
25. Jafarian M, Mahjani M G, Gobal F, Danaee I. Effect of potential on the early stage of nucleation and growth during aluminum electrocrystallization from molten salt ($AlCl_3$-NaCl-KCl). Journal of Electroanalytical Chemistry, 2006, 588(2): 190–196
26. Moffat T P. Electrodeposition of Al-Cr metallic glass. Journal of the Electrochemical Society, 1994, 141(9): L115–L117
27. Ding Z M, Feng Q Y, Shen C B, Gao H. Rule of formation of aluminum electroplating layer on Q235 steel. Journal of Environmental Sciences (China), 2011, 23: S138–S141
28. Nayak B, Misra M M. The electrodeposition of aluminium on brass from a molten aluminium chloride-sodium chloride bath. Journal of Applied Electrochemistry, 1977, 7(1): 45–50
29. Li Q F, Hjuler H A, Berg R W, Bjerrum N J. Electroless growth of aluminum dendrites in NaCl-$AlCl_3$ melts. Journal of the Electrochemical Society, 1989, 136(10): 2940–2943
30. Jiang L, Jin Z, Xu F, Yu Y, Wei G, Ge H, Zhang Z, Cao C. Effect of potential on aluminium early-stage electrodeposition onto NdFeB magnet. Surface Engineering, 2017, 33(5): 375–382
31. Fellner P, Chrenková-Paučírová M, Matiašovský K. Electrolytic aluminum plating in molten salt mixtures based on $AlCl_3$. I: Influence of the addition of tetramethylammonium chloride. Surface Technology, 1981, 14(2): 101–108
32. Liu L, Lu X M, Cai Y J, Zheng Y, Zhang S J. Influence of additives on the speciation, morphology, and nanocrystallinity of aluminium electrodeposition. Australian Journal of Chemistry, 2012, 65(11): 1523–1528
33. Miyake M, Kubo Y, Hirato T. Hull cell tests for evaluating the effects of polyethylene amines as brighteners in the electrodeposition of aluminum from dimethylsulfone-$AlCl_3$ baths. Electrochimica Acta, 2014, 120: 423–428
34. Zhang Q Q, Wang Q, Zhang S J, Lu X M. Effect of nicotinamide on electrodeposition of Al from aluminium chloride ($AlCl_3$)-1-butyl-3-methylimidazolium chloride ([Bmim]Cl) ionic liquids. Journal of Solid State Electrochemistry, 2014, 18(1): 257–267
35. Wang Q, Zhang Q Q, Chen B, Lu X M, Zhang S J. Electrodeposition of bright Al coatings from 1-butyl-3-methylimidazolium chloroaluminate ionic liquids with specific additives. Journal of the Electrochemical Society, 2015, 162(8): D320–D324
36. Howie R C, Macmillan D W. The electrodeposition of aluminium from molten aluminium chloride/sodium chloride. Journal of Applied Electrochemistry, 1972, 2(3): 217–222
37. Li Q F, Hjuler H A, Berg R W, Bjerrum N J. Electrochemical deposition and dissolution of aluminum in $NaAlCl_4$ melts influence of $MnCl_2$ and sulfide addition. Journal of the Electrochemical Society, 1990, 137: 2794–2798
38. Jafarian M, Mahjani M G, Gobal F, Danaee I. Electrodeposition of aluminum from molten $AlCl_3$-NaCl-KCl mixture. Journal of Applied Electrochemistry, 2006, 36(10): 1169–1173
39. Delimarsky Y K, Tumanova N K. A study of the effect of surfactants on electrode processes in molten salts. Electrochimica Acta, 1979, 24(1): 19–24
40. Paučírová M, Matiašovský K. Electrolytic aluminium-plating in fused salts based on chlorides. Electrodeposition and Surface Treatment, 1975, 3(2): 121–128
41. Bakkar A, Neubert V. Electrodeposition and corrosion characterisation of micro- and nano-crystalline aluminum from $AlCl_3$/1-ethyl-3-methylimidazolium chloride ionic liquid. Electrochimica Acta, 2013, 103: 211–218
42. Li M, Gao B L, Chen W T, Liu C Y, Wang Z W, Shi Z N, Hu X W. Electrodeposition behavior of aluminum from urea-acetamide-lithium halide low-temperature molten salts. Electrochimica Acta, 2013, 185: 148–155
43. Li M, Gao B L, Shi Z N, Hua X W, Wang S X, Li L X, Wang Z W, Yu J Y. Electrochemical study of nickel from urea-acetamide-LiBr low-temperature molten salt. Electrochimica Acta, 2015, 169: 82–89
44. Abbott A, Barron J C, Frisch G, Ryder K, Silva A F S. The effect of additives on zinc electrodeposition from deep eutectic solvents. Electrochimica Acta, 2011, 56(14): 5272–5279
45. Tsuda T, Nohira T, Ito Y. Nucleation and surface morphology of aluminum-lanthanum alloy electrodeposited in a $LaCl_3$-saturated$AlCl_3$-EtMeImCl room temperature molten salt. Electrochimica Acta, 2002, 47(17): 2817–2822
46. Liao Q, Pitner W R, Stewart G, Hussey C, Stafford G R. Electrodeposition of aluminum from the aluminum chloride-1-methyl-3-ethyl imidazolium chloride room temperature molten salt + benzene. Journal of the Electrochemical Society, 1997, 144(3): 936–943